Polymer Journal (2015) 47, 464–467

www.nature.com/pj

NOTE

# Chain architecture and flexibility of α-cyclodextrin/PEG polyrotaxanes in dilute solutions

Shimpei Yamada[1], Yusuke Sanada[1], Atsushi Tamura[2], Nobuhiko Yui[2] and Kazuo Sakurai[1]

*Polymer Journal* (2015) **47,** 464–467; doi:10.1038/pj.2015.18; published online 22 April 2015

## INTRODUCTION

Supramolecular chemistry adopts a unique strategy to build molecules at nanolevel using various intermolecular interactions. Supramolecular chemistry is now merging with macromolecular chemistry to create a new field, which can be called 'supra-macromolecular' chemistry.[1] Harada *et al.*[2] have extensively studied a series of polyrotaxanes (PRXs) composed of cyclodextrins (CD) and various linear polymers, including poly(ethylene glycol) (PEG). Several α-CDs are spontaneously threaded onto a PEG chain to form pseudopolyrotaxanes in aqueous solutions.[3] When both ends of the PEG in pseudopolyrotaxanes are capped by a bulky molecule, α-CDs are trapped on the PEG chain.[2,3] Heavily α-CD-threaded PRXs are expected to have a rod-like nature because the threaded α-CDs should reduce the flexibility of the PEG chain.

Yui and colleagues[4,5] have studied the biomaterial application of PRXs such as a delivery carrier for genes or proteins using their unique supramolecular functions, which include the stimuli-induced dissociation through the cleavage of terminal bulky stoppers and the freely mobile nature of threading CDs along the polymer chain. In some cases, an increase in the number of threading CDs in PRXs is a predominant factor to enhance the physicochemical stability of polyelectrolyte complexes with nucleic acids and their intracellular uptake efficiency.[5] These results indicate the importance of the conformation of PRXs chains.

Although the rod-like architecture of PRXs has been directly observed with scanning probe microscopy, its quantitative analysis has not been fully investigated.[6] Additionally, although the conformation of PRXs and the dynamic motion of α-CDs along the PEG axle have been investigated using small-angle neutron scattering in organic solvents,[7] the relationship between the conformation of PRXs and the threading percentage of α-CDs in aqueous solutions has not been clarified except for measuring the radius of gyration as a function of the molecular weight.[8] This study examines the dilute solution properties of a series of water-soluble PEG/α-CD PRXs with different numbers of threading α-CDs in aqueous media using small-angle X-ray scattering (SAXS) to determine the persistence length ($p$) and other molecular characteristics for the worm-like cylinder model.

## EXPERIMENTAL PROCEDURE

Three α-CD/PEG PRXs, which were capped with *N*-benzyloxycarbonyl-L-tyrosine with different threading percentages of α-CD ($\varphi_{CD}$), were synthesized by varying the feed [α-CD]/[PEG] ratio using PEG with $M_w = 1.15 \times 10^4$ g mol$^{-1}$ as an axle polymer (Supplementary Scheme S1), as listed in Table 1. The number of threading α-CDs in PRXs was determined using $^1$H NMR, and the values of $\varphi_{CD}$ were determined by assuming that one α-CD includes two ethylene glycol with repeating units of PEG (Supplementary Figures S1–S3). To obtain the solubility in aqueous solution, hydrophilic hydroxyethoxy ethyl (HEE) groups were chemically modified on the α-CD moieties in PRXs (HEE–PRX), and the number of modified HEE groups on PRXs is listed in Table 1. The weight-averaged molecular weight ($M_w$) and polydispersity index ($M_w/M_n$) of HEE–PRX were determined using static light scattering coupled with size exclusion chromatography (SEC). The fully stretched length ($L_f$), that is, the contour length of the PEG chain, was calculated based on the repeating unit length of 0.34 nm.

## RESULTS AND DISCUSSION

Figure 1a shows the SAXS profiles from 25CD with different concentrations. The SAXS intensity is a function of the concentration ($c$) and the magnitude of the scattering vector ($q$); thus, it may be expressed as $I(q, c)$. To eliminate intermolecular scattering, $I(q, c \to 0)$ was evaluated by extrapolating the obtained $I(q, c)$ to $c \to 0$ as shown in Figure 1b. The resultant $[I(q,c)/c]_{c \to 0}$, which is hereinafter denoted by $I(q)$, only contains the intramolecular scattering, which is called the form factor. In Figure 1a, for convenience, $I(q)$ was shifted from the others by multiplying by 10. In the low-$q$ region, the relation of $0 < \alpha < 1$ was held, where $\alpha$ is defined by $I(q) \propto q^{-\alpha}$; with an increase in $q$, the value of $\alpha$ became $\alpha \sim 1$ in the middle-$q$ range. Further increase of $q$ made $1 < \alpha$ in the high-$q$ region. This result is a typical scattering behavior from semi-flexible polymer chains with a relatively short contour length.[9] Therefore, it is reasonable to presume that the HEE-group-modified PEG/α-CD PRXs behave similarly to a semi-flexible short chain. The best model to describe the dilute solution

[1]Department of Chemistry and Biochemistry, The University of Kitakyushu, Fukuoka, Japan and [2]Department of Organic Biomaterials, Institute of Biomaterials and Bioengineering, Tokyo Medical and Dental University, Tokyo, Japan
Correspondence: Professor K Sakurai, Department of Chemistry and Biochemistry, The University of Kitakyushu, 1-1 Hibikino, Wakamatsu, Kitakyushu, Fukuoka 808-0135, Japan.
E-mail: sakurai@kitakyu-u.ac.jp
Received 6 January 2015; revised 13 February 2015; accepted 16 February 2015; published online 22 April 2015

**Table 1 Molecular characteristics of α-cyclodextrin rotaxane**

| *Sample codes* | *Number of α-CD* | $\varphi_{CD}$ *(%)* | *Number of HEE groups*[a] | $M_{n,NMR} \times 10^{-4}$[b] *(g mol$^{-1}$)* | $M_w \times 10^{-4}$[c] *(g mol$^{-1}$)* | $M_w/M$[c] | $L_f$ *(nm)* |
|---|---|---|---|---|---|---|---|
| PEG-OH | — | — | — | 0.98 | 1.15 | 1.01 | 89.2 |
| 25CD | 27.7 | 24.9 | 91.7 (3.31) | 4.97 | 8.55 | 1.01 | — |
| 34CD | 37.8 | 34.0 | 126.3 (3.34) | 6.41 | 10.9 | 1.02 | — |
| 50CD | 55.8 | 50.1 | 210.4 (3.77) | 9.26 | 12.4 | 1.01 | — |

Abbreviations: CD, cyclodextrins; HEE, hydrophilic hydroxyethoxy ethyl; PEG, poly(ethylene glycol); SEC, size exclusion chromatography.
[a]Values in the parenthesis are averaged number of HEE groups on single α-CD in polyrotaxane.
[b]Determined by $^1$H NMR.
[c]Determined by SEC-multiangle light scattering.

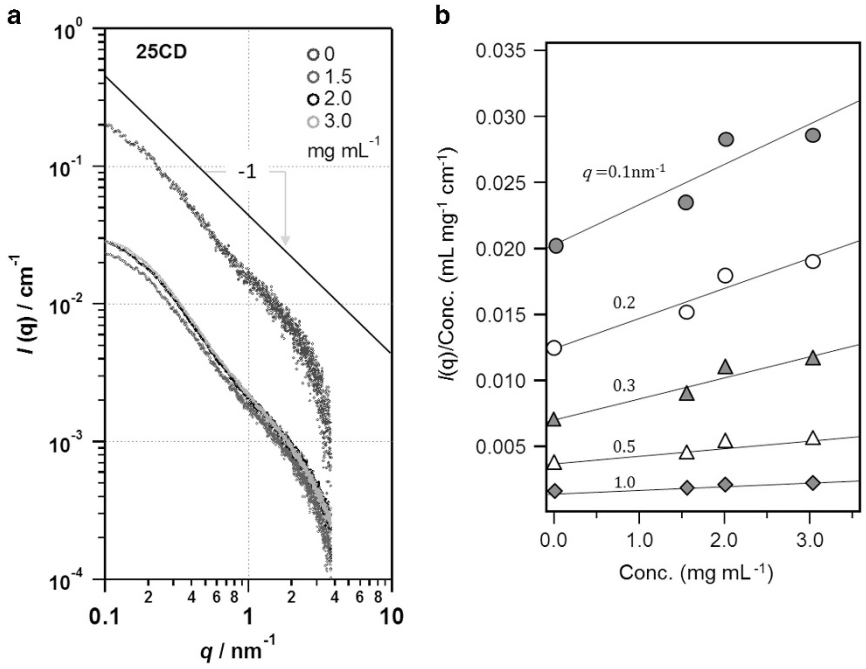


**Figure 1** (**a**) Small-angle X-ray scattering profiles for three different concentrations and the extrapolated profile at the zero concentration (shifted upward by multiplying with a factor of 10). (**b**) Concentration dependences of $I(q)$ for the five selected $q$ values. A full color version of this figure is available at *Polymer Journal* online.

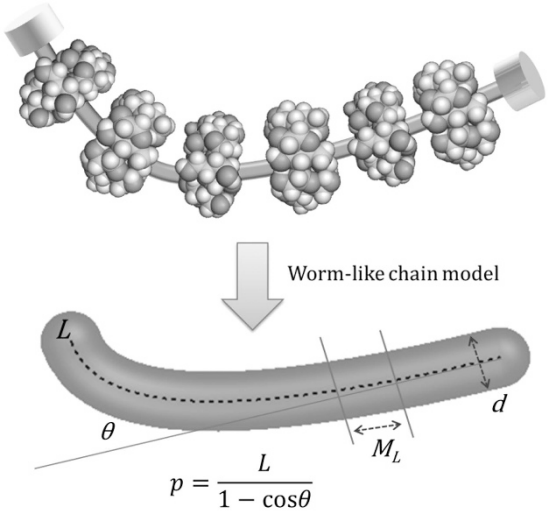


**Figure 2** End-capped α-cyclodextrin/poly(ethylene glycol) polyrotaxane and a corresponding worm-like chain model to describe its dilute solution properties. A full color version of this figure is available at *Polymer Journal* online.

properties including SAXS for this system is the worm-like cylinder model.[10]

As illustrated in Figure 2, we regard the HEE group-modified PEG/α-CD PRXs as a worm-like cylinder with a set of four parameters: the contour length $L$, cylinder diameter $d$, molar mass per unit length $M_L$, and persistence length $p$. Here, the axis of the worm-like cylinder is expressed in terms of Kratky–Porod chain statistics. The form factor for worm-like cylinders may be expressed by:

$$I(q)/c = L^2 \int_0^L (L-x) F\left(\overrightarrow{q};x\right) \mathrm{d}x \qquad (1)$$

Here, $F\left(\overrightarrow{q};x\right)$ can be expressed as the Fourier transform of the probability density function, where the contour point $x$ is found at a specified point $\overrightarrow{r}$ (which can be related to $\overrightarrow{q}$) and may be expanded with the moments $\left\langle \overrightarrow{r}^{2n} \right\rangle$. Nakamura and Norisuye[11] calculated these moments for the Kratky–Porod chain[12] and obtained a series of numerical tables, which allow us to calculate the form factor for the entire $q$ range as a function of $q$, $p$, $L$ and $d$.

There are two types of plots to examine how well the experimental data points are fitted by the theoretical values, which were calculated from equation (1): the Kratky ($I(q)q^2$ vs $q$) and Holtzer ($I(q)q$ vs $q$)

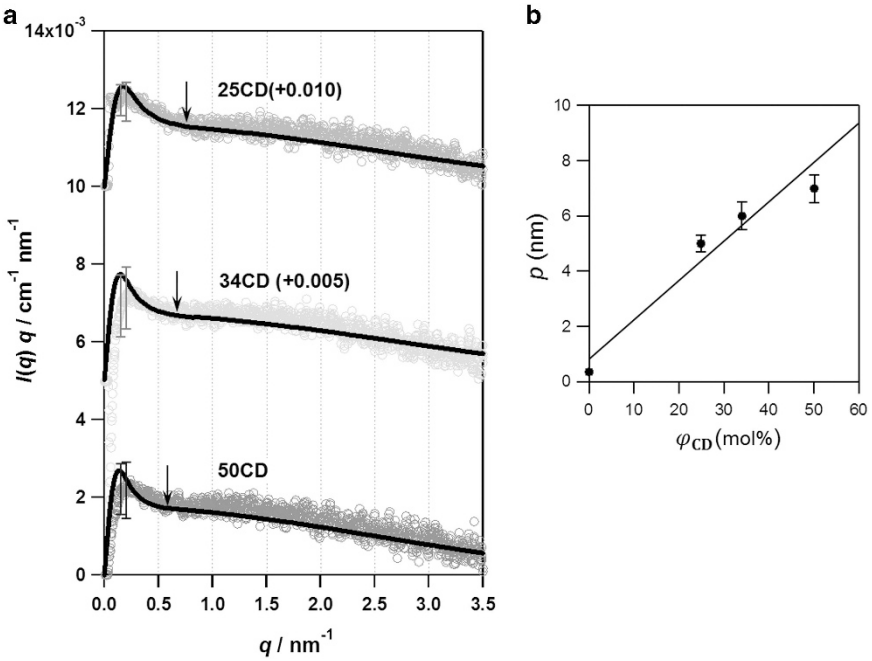


**Figure 3** (**a**) Holtzer plots for three samples and the best-fit curves, which were calculated from the Norisuye–Nakamura's theory. (**b**) α-Cyclodextrin loading dependence of the obtained persistence length. A full color version of this figure is available at *Polymer Journal* online.

**Table 2 Molecular characteristics of α-cyclodextrin rotaxane**

| | $R_g$ *(nm)* | $M_L$ *(g mol$^{-1}$ nm$^{-1}$)* | d *(nm)* | L *(nm)* | p *(nm)* | $R_a$ |
|---|---|---|---|---|---|---|
| 25CD | 10.7 | 1550±100 | 1.1±0.1 | 55.1±2.0 | 5.0±0.5 | 4.5 |
| 34CD | 12.5 | 1700±150 | 1.2±0.1 | 64.3±2.5 | 6.0±0.5 | 5.0 |
| 50CD | 13.4 | 1800±100 | 1.2±0.1 | 66.8±2.2 | 7.0±0.5 | 5.8 |

Abbreviation: CD, cyclodextrins.

plots. Because the Holtzer plots are good for short chains, we adopted this type of plot. Figure 3a compares the data and best-fitted curves for three samples. It can be concluded that the entire scattering data were well fitted by the worm-like cylinder model for a suitable set of parameters. The obtained parameter sets are summarized in Table 2, and Figure 3b shows the persistence length versus $\varphi_{CD}$ and that for PEG.[13] As expected, with an increase in $\varphi_{CD}$, the rigidity increases; however, their increments are less significant than expected in comparison with that of PEG. After dividing $L$ with the diameter $d$, the axial ratio ($R_a$) was obtained and listed in the 7th column in Table 2. When we compare this value with typical semi-flexible chains such as schizophyllan (153),[14,15] poly(*n*-hexyl isocyanate) (46),[16] sodium hyaluronate (8.2)[17] and a polystyrene polymacromonomer (3-4),[9] the present system has a similar flexibility to those of polystyrene polymacromonomer and cylindrical lipid micelles.[18]

During our iteration process to fit the data, we had to choose a shorter $L$ than that of the PEG chain template. As shown in Figure 3a, we did not observe a clear Guinier region (that is, $I(q) \propto q^{-0}$ at the lower $q$, and with increasing $q$, $I(q) \propto \exp(-\frac{4}{3}R_g^2 q^2)$, where $R_g$ is the radius of gyration). Therefore, we must admit that our fitting is not sensitive to the magnitude of $L$, although we did not obtain a better fitting using an identical $L$ with the original PEG chain (Supplementary Figure S4). Note that the value of $L$ to give the best fitting is less than the original PEG chain length. Compared with $L$, SAXS enabled us to accurately determine $d$, and the obtained values were close to the diameter of α-CD, which shows that the determined parameters were notably reasonable.

Figure 4 compares $M_w$ dependence of the intrinsic viscosity ($[\eta]$) for the template PEG and three PRX samples, where $[\eta]$ was determined with a viscometer coupled with SEC. The curve with the identical color and plotted mark represents the calculated $L$ dependence of $[\eta]$ values with the identical $p$, $M_w$ and $d$, which were determined by SAXS for each sample. Compared with the data and the calculated lines, the parameters determined by SAXS can well produce the $[\eta]$ values. Here, the curves of the PRX were calculated using Yamakawa–Fujii's theory,[19] and the curve of PEG was produced using a Mark–Houwink–Sakurada relation for PEG.[20] Supposing that a PRX has the identical $\varphi_{CD}$ with 25CD and its $L$ is identical to that of the template PEG, the value of $[\eta]$ should be 42.0 cm$^3$ g$^{-1}$, as plotted with the cubic mark. This value is notably larger than the measured value, which confirms the SAXS results that $L$ becomes shorter upon complexation with α-CD. The identical calculation was performed for the other samples, and the resulting values are plotted in Figure 4. The reason for this change is not clear, but we can presume that the time scale difference between PEG chain reputations and α-CD thermal motion may cause the PEG chain to dangle between the adjacent chains.

## CONCLUSION

In summary, SAXS was performed for three HEE group-modified PEG/α-CD PRXs with different $\varphi_{CD}$ values that were made from the same template PEG, and the data were analyzed using the worm-like cylinder model. The results show that the chain flexibility, which is expressed by $p$, increases with an increase in $\varphi_{CD}$; however, its increment is not larger than normally expected. The chain flexibility is in the almost identical range with polystyrene polymacromonomer or cylindrical lipid micelles. The contour length of PRX becomes shorter by ~30% compared with the template PEG after the inclusion

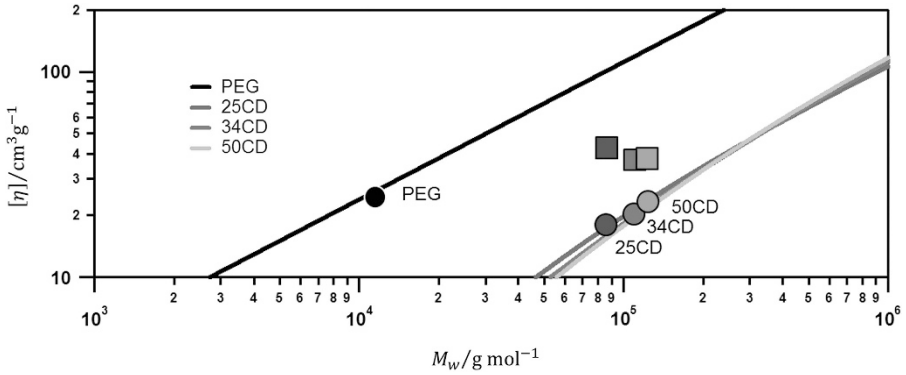


**Figure 4** Intrinsic viscosities *vs* the molecular weight for the three polyrotaxane samples and poly(ethylene glycol) and the comparison with the theoretically calculated values from the Yamakawa–Fujii equation with the identical $p$, $M_L$ and $d$. A full color version of this figure is available at *Polymer Journal* online.

complex formation with α-CDs, which was confirmed by the viscosity measurements.

## ACKNOWLEDGEMENTS

A part of this work was financially supported by the Grant-in-Aid for Scientific Research (No. 23107004) on Innovative Areas 'Nanomedicine Molecular Science' (No. 2306) from the Ministry of Education, Culture, Sports, Science, and Technology (MEXT) of Japan. All SAXS measurements were performed at SPring-8 40B2(2014A1268).

1 Schultz, A., Li, X., Barkakaty, B., Moorefield, C. N., Wesdemiotis, C. & Newkome, G. R. Stoichiometric self-assembly of isomeric, shape-persistent, supramacromolecular bowtie and butterfly structures. *J. Am. Chem. Soc.* **134**, 7672–7675 (2012).
2 Harada, A., Hashidzume, A., Yamaguchi, H. & Takashima, Y. Polymeric rotaxanes. *Chem. Rev.* **109**, 5974–6023 (2009).
3 Harada, A., Li, J. & Kamachi, M. The molecular necklace: a rotaxane containing many threaded [alpha]-cyclodextrins. *Nature* **356**, 325–327 (1992).
4 Ooya, T. & Yui, N. Synthesis and characterization of biodegradable polyrotaxane as a novel supramolecular-structured drug carrier. *J. Biomater. Sci., Polym. Ed.* **8**, 437–455 (1997).
5 Tamura, A. & Yui, N. Cellular internalization and gene silencing of siRNA polyplexes by cytocleavable cationic polyrotaxanes with tailored rigid backbones. *Biomaterials* **34**, 2480 (2013).
6 Shigekawa, H., Miyake, K., Sumaoka, J., Harada, A. & Komiyama, M. The molecular abacus: STM manipulation of cyclodextrin necklace. *J. Am. Chem. Soc.* **122**, 5411–5412 (2000).
7 Mayumi, K., Osaka, N., Endo, H., Yokoyama, H., Sakai, Y., Shibayama, M. & Ito, K. Concentration-induced conformational change in linear polymer threaded into cyclic molecules. *Macromolecules* **41**, 6480–6485 (2008).
8 Fleury, G., Brochon, C., Schlatter, G., Bonnet, G., Lapp, A. & Hadziioannou, G. Synthesis and characterization of high molecular weight polyrotaxanes: towards the control over a wide range of threaded α-cyclodextrins. *Soft Matter* **1**, 378–385 (2005).
9 Terao, K., Nakamura, Y. & Norisuye, T. Solution properties of polymacromonomers consisting of polystyrene. 2. chain dimensions and stiffness in cyclohexane and toluene. *Macromolecules* **32**, 711–716 (1999).
10 Yamakawa, H. *Modern Theory of Polymer Solutions* (Harper & Row, New York, NY, USA, 1971).
11 Nakamura, Y. & Norisuye, T. Scattering function for wormlike chains with finite thickness. *J. Polym. Sci. Part B: Polym. Phys.* **42**, 1398–1407 (2004).
12 Kratky, O. & Porod, G. Röntgenuntersuchung gelöster Fadenmoleküle. *Recueil des Travaux Chimiques des Pays-Bas* **68**, 1106–1122 (1949).
13 Kienberger, F., Pastushenko, V. P., Kada, G., Gruber, H. J., Riener, C., Schindler, H. & Hinterdorfer, P. Static and dynamical properties of single poly(ethylene glycol) molecules investigated by force spectroscopy. *Single Mol.* **1**, 123–128 (2000).
14 Yanaki, T., Norisuye, T. & Fujita, H. Triple helix of schizophyllum commune polysaccharide in dilute solution. 3. hydrodynamic properties in water. *Macromolecules* **13**, 1462–1466 (1980).
15 Kashiwagi, Y., Norisuye, T. & Fujita, H. Triple helix of Schizophyllum commune polysaccharide in dilute solution. 4. Light scattering and viscosity in dilute aqueous sodium hydroxide. *Macromolecules* **14**, 1220–1225 (1981).
16 Okamoto, N., Mukaida, F., Gu, H., Nakamura, Y., Sato, T., Teramoto, A., Green, M. M., Andreola, C., Peterson, N. C. & Lifson, S. Molecular weight dependence of the optical rotation of poly((R)-1-deuterio-n-hexyl isocyanate) in dilute solution. *Macromolecules* **29**, 2878–2884 (1996).
17 Ribeiro, W., Mata, J. L. & Saramago, B. Effect of concentration and temperature on surface tension of sodium hyaluronate saline solutions. *Langmuir* **23**, 7014–7017 (2007).
18 Naruse, K., Eguchi, K., Akiba, I., Sakurai, K., Masunaga, H., Ogawa, H. & Fossey, J. S. Flexibility and cross-sectional structure of an anionic dual-surfactant wormlike micelle explored with small-angle X-ray scattering coupled with contrast variation technique. *J. Phys. Chem. B* **113**, 10222–10229 (2009).
19 Yamakawa, H. & Fujii, M. in *Macromolecules* Vol. 7, 649–654 (American Chemical Society, 1974).
20 Mendichi, R., Rizzo, V., Gigli, M. & Schieroni, A. G. Fractionation and characterization of a conjugate between a polymeric drug-carrier and the antitumor drug camptothecin. *Bioconjug. Chem.* **13**, 1253–1258 (2002).

Supplementary Information accompanies the paper on Polymer Journal website (http://www.nature.com/pj)